Mathematical Analysis in Characterization of Carbon Nanotubes (CNTs) as possible Mosquito Repellents

Viktor Andonovic
Jožef Stefan Institute, Slovenia
Mimoza Kovaci Azemi
Faculty of Technology and Metallurgy, North Macedonia
Beti Andonovic
Faculty of Technology and Metallurgy, North Macedonia
Aleksandar T. Dimitrov
Faculty of Technology and Metallurgy, North Macedonia

Abstract

Mosquitoes are a great threat to human health to date and are a subject of interdisciplinary research involving scientists from many areas. Recently much attention has been put to novel approaches to mosquito repellent products that involve the use of novel materials, such as carbon nanomaterials, where it is essential to determine their properties. This research discusses the full molecular characterization of carbon nanotubes (CNTs) produced by electrolysis in molten salts. Each CNT has its mathematical representation due to its hexagonal lattice structure. Multi-wall carbon nanotubes (MWCNTs) are considered. The focus is on determining their structural parameters: innermost and outermost diameters, chiral indices m and n, number of walls, and unit cell parameters. Corresponding frequency parts of Raman spectra of four experimentally produced CNTs are elaborated, and Python programming and Mathematica are employed for the most accurate (m,n) assignment. Determining the chirality of these samples enables the calculation of other structural properties, which are performed now, including their graph representation. The latter enables the evaluation of different distance-based topological indices (Wiener, Balaban, Sum-Balaban, Harary index, etc.) to predict some index-related properties of the molecules.

Keywords: CNT; electrolysis; graphite; molten salts; topological indices; Python
JEL classification: C61, O31, L61
Acknowledgments: This research is based upon work from COST Action CA 16227, "Investigation and Mathematical Analysis of Avant-garde Disease Control via Mosquito Nano-Tech-Repellents," supported by COST (European Cooperation in Science and Technology).

Paper type: Research article
Received: 15 Mar 2022
Accepted: 08 May 2022

DOI: 10.54820/entrenova-2022-0004

Introduction

Carbon nanotubes (CNTs) are one of the several allotropes of carbon in nano dimensions (1 nm = 10^{-9} m) with highly outstanding properties. Since graphene is a 2D building unit of all carbon allotropes such as fullerenes, CNTs, nanoribbons, and so on, CNTs may be geometrically observed as wrapped-up graphene structures having a seamless cylindrical shape. Each nanotube has its mathematical representation due to its hexagonal lattice structure (Dresselhaus et al., 2005; Zhao et al., 2002). The geometric structure analysis of carbon nanotubes has been quite a challenging task, particularly if the subject of research is multi-wall carbon nanotubes (MWCNTs) (Dresselhaus et al., 2005; Zhao et al., 2002; Schwandt et al., 2012; Natsuki et al., 2013; Benoit et al., 2002; Andonovic et al., 2020). Knowing CNT's structural parameters (diameter, chiral angle, chiral indices *m* and *n*) is knowing their properties, which is essential for any research in the field of CNTs and their application for a variety of wearable technologies to provide advanced functions that include sensing, temperature regulation, chemical, mechanical, or radioactive protection, or energy storage. Recently an important application field has been added, due to certain mosquitos' repellent properties of CNTs and other carbon nanomaterials, such as applications in waste water treatment, textile, etc. Such materials offer an additional unanticipated function: mosquito bite protection for light, fiber-based fabrics. There is a fundamental interaction between CNT-based films and the globally important mosquito species Aedes aegypti, through live mosquito experiments, needle penetration force measurements, and mathematical modeling of mechanical puncture phenomena. Successful application of CNTs and other carbon nanomaterials as potential mosquito repellents may follow thorough research, including successful characterization of the produced carbon nanomaterials.

Several excellent tools, such as HRTEM, ED, RRS, and others, suggest some models of (*m*, *n*) assignment for single-wall carbon nanotubes (SWCNTs) and for MWCNTs. However, precise determination of the CNT's molecular structure features becomes extremely complicated for multi-walled tubes, even when there are just a few walls (layers) (Natsuki et al., 2013; Benoit et al., 2002). Thorough and overall analysis and use of experimental results combined with the recent theoretical background may lead to successful estimation of its structural elements.

There are different experimental methods of producing CNTs, and based on several factors, the obtained tubes may be either SWCNTs or MWCNTs. The CNT with the lowest reported diameter value experimentally produced is known to have the diameter $d_k = 4\text{Å}$. It is the narrowest attainable nanotube that can remain energetically stable. In contrast to CNTs with larger diameters, whose conductivity nature depends on their chirality, these smallest nanotubes are always metallic, regardless of the chirality (Qin et al., 2000).

In chemical graph theory, QSAR and QSPR have often used terms derived from Quantitative Structure-Property Relations and Quantitative Structure-Activity Relations. QSAR and QSPR are regression models that relate a set of "predictor" variables to the power of the response variable.

In QSAR modeling, the predictors consist of Physico-chemical properties or theoretical molecular descriptors of chemicals, while the QSAR response variable could be a biological, pharmacological, medical, ecological, and/or some other activity of the chemicals.

Both QSAR and QSPR show the tendency of contemporary theoretical and mathematical chemistry to predict the properties of a compound based on its

molecule structure. The research in this field is mainly done by combining molecular graph descriptors and experimental results. They use a simple method of representing molecules/structures as graphs. Each atom is presented as a vertex; the bonds between the atoms are the edges (links) in the graph.

In what follows, let G be a connected graph. By $V(G)$ and $E(G)$ the vertex and edge set of G are respectively denoted. Let $k=|V(G)|$ and $e=|E(G)|$. Two vertices $u,v\in V(G)$ being given $dist(u,v)$ is the distance from u to v in G. This paper only considers distance-based topological indices such as the Wiener index, Harary index, Gutman index, Balaban index, and Sum-Balaban index.

The Wiener index is historically the first topological index. Wiener introduced it (Wiener, 1947) and defined it as the sum of distances between all pairs of vertices. Hence, for a graph, G the Wiener index $W(G)$ is

$$W(G)=\sum_{u,v\in V(G)} dist(u,v) \qquad (1.1)$$

This index is widely studied in chemistry and in pure mathematics. It has also found applications in sociometry and the theory of social networks. Based on the success of the Wiener index, plenty of molecular descriptors have been developed afterward.

The Harary index of a graph is defined as

$$H(G)=\sum_{u,v\in V(G)} \frac{1}{dist(u,v)} \qquad (1.2)$$

where the sum is over all pairs of distinct vertices of G. This index was introduced independently by Plavšić et al. and by Ivanciuc et al. in 1993. It turned out that the performance of this index for chemical purposes is quite modest, but on the other side, the Harary index also appears in the study of complex networks.

The Balaban index was introduced by Balaban (Balaban, 1982,1983). This topological index was used successfully in QSAR/QSPR modeling (Devillers et al., 1999; Grassy et al., 1998; Khadikar et al., 2004). The Balaban index $J(G)$ of a graph G is defined as:

$$J(G)=\frac{e}{e-k+2}\sum_{uv\in E(G)} \frac{1}{\sqrt{w(u)w(v)}} \qquad (1.3)$$

where the sum is over all edges uv of G. For $x\in V(G)$, we have

$$w(x)=\sum_{y\in V} dist(x,y) \qquad (1.4)$$

In (Balaban, 2002), it was shown that the Balaban index reduces the degeneration of the Wiener index for alkanes and provides a much higher discriminating ability. Therefore, the Balaban index is also called the "sharpened Wiener index."

The Sum-Balaban index is a recently introduced modification of the Balaban index, and it is defined as:

$$SJ(G)=\frac{e}{e-k+2}\sum_{uv\in E(G)} \frac{1}{\sqrt{w(u)+w(v)}} \qquad (1.5)$$

The Gutman index is another distance-based topological index defined as

$$Gut(G)=\sum_{u,v\in V(G)} d(u)d(v)dist(u,v) \qquad (1.6)$$

The results relevant to CNTs topological indices are motivated by (Andova et al., 2016), where the number of vertices at a given distance from a vertex u on an infinite hexagonal tube is determined. According to these results, the asymptotic value of Wiener, Gutman, Balaban, Sum-Balaban, and Harary indices for nanotubes are obtained.

Both lower and higher frequency Raman spectra are discussed of three experimentally produced CNTs of undetermined diameter, chirality, and the number of walls, and the higher frequency Raman spectrum of one MWCNT. The first three are assigned the following nomenclatures: CNT_1, CNT_2, and CNT_3, whereas the fourth is assigned the CNT-3 nomenclature. Since their properties are tightly connected and dependent on their atomic structure, detailed analyses concerning determining their diameters are performed, as well as calculating their chiral indices *m* and *n*, and other parameters, hence estimating the number of walls of each of the first three nanotubes. This research was strictly focused on determining the outermost and innermost diameters, assigning the corresponding chiral indices to the tubes' walls, and estimating the number of other inner diameters, which would further implicate the number and the conductive nature of the walls. It is strongly suggested to perform future studies on the samples, as are additional EDP analyses to enhance and confirm the accuracy of applied methods and estimation of distance-based topological indices (Wiener, Harary, Balaban, Sum-Balaban, Gutman, etc.) of all samples. Their estimation is possible by using the graph representation and the chirality of the studied samples. The latter is performed for the nanotube CNT-3, following its outermost diameter estimation and discussion. The distance-based topological indices are known to be related to some properties of the corresponding molecules, which is a valuable fact regarding their application, including the application of mosquito-repellent products.

Methodology

CNT samples subject to this research are obtained by electrolysis in molten salts using non-stationary current regimes. Lithium chloride and sodium chlorite are used as molten salts. As a result of Li or Na intercalation into the graphite and thus its exfoliation, CNTs are obtained. The morphological structures of the nanotubes were investigated by TEM analysis using an FEI Tecnai G2 Spirit TWIN with a LaB6 cathode. The nanotubes were observed by scanning electron microscopy using JEOL 6340F (SEM, 10 kV). Structural characteristics of the carbon nanostructures were studied through Raman spectroscopy. Non-polarized Raman spectra were recorded by a confocal Raman spectrometer (Lab Ram ARAMIS, Horiba Jobin Yvon) operating with a laser excitation source emitting at 532 nm. The low-frequency regions 50-350 cm^{-1} were taken into consideration, as well as the frequency regions 1200-1800 cm^{-1} from the Raman spectra of the CNTs. Python programming was applied to determine possible chiral indices assignment to the studied CNT_1, CNT_2, and CNT_3 samples. The software Mathematica was applied to determine possible chiral indices assignment to the CNT-3 sample.

The general equations used for determining the CNTs structures are used as follows:

$$\left|\vec{C}_h\right| = \sqrt{3}a_{C-C}(m^2 + mn + n^2)^{1/2} \text{ nm} \quad (2.1)$$

$$d_{CNT} = \frac{\sqrt{3}a_{C-C}(m^2 + mn + n^2)^{1/2}}{\pi} = 0.079\sqrt{(m^2 + mn + n^2)} \text{ nm} \quad (2.2)$$

$$\theta = arctg\frac{\sqrt{3}n}{2m+n},$$
$$0 \le \theta \le \frac{\pi}{6} \quad (0 \le n \le m) \quad (2.3)$$

$$T = \left|\vec{T}\right| = \frac{\sqrt{3}\left|\vec{C}_h\right|}{d_R} = \frac{\sqrt{3}\pi d_{CNT}}{d_R} \text{ nm}, \quad (2.4)$$
$$d_R = GCD(2m+n, 2n+m), \quad \text{given by}$$
$$d_R = \begin{cases} d, & \text{if } m-n \text{ is not a multiple of } 3d \\ 3d, & \text{if } m-n \text{ is a multiple of } 3d \end{cases}$$
$$\text{where } d = \text{GCD}(m,n)$$

$$N_{\text{H}} = \frac{2(m^2+mn+n^2)}{d_R} \quad (2.5)$$
$$N_{\text{V}} = \frac{4(m^2+mn+n^2)}{d_R}$$

$$d_i = \frac{228}{\omega_i^{RBLM}} \quad (2.6)$$
$$d_o = \frac{228}{\sqrt{(\omega_o^{RBLM})^2 - 228^2 \cdot C_e}},$$
$$C_e = 0.065 \text{ nm}^{-2}$$

$$\omega_{RBM} = \frac{A}{d} + B \quad (2.7)$$
$$A = 223 \text{ cm}^{-1}, \quad B = 10 \text{ cm}^{-1}$$

$$\omega_{TO}^{G}(d) = 1582 - \frac{27.5}{d^2}, \quad \text{for SC} \quad (2.8)$$

$$\omega_{LO}^{G}(d) = 1582 - \frac{38.8}{d^2}, \quad \text{for MC} \quad (2.9)$$

For a mathematical representation of CNTs and due to its hexagonal lattice atomic structure, one can use the relations among various CNT parameters reported in numerous works, as are (Dresselhaus et al. 2005): unit vectors $\vec{a}_1$ and $\vec{a}_2$, chiral vector $\vec{C}_h$, CNT diameter d_{CNT}, chiral angle θ, translation vector $\vec{T}$ of the CNT unit cell (being the shortest repeat distance along the nanotube axis), number of hexagons N_H, number of vertices (atoms) N_V and so on, which are expressed with the formulas (2.1)-(2.5) in the experimental part. Lattice constants are the lengths of the

unit vectors $a = |\vec{a}_1| = |\vec{a}_2| = 0.246\ \text{nm}$ and the distances between neighboring carbon atoms are $a_{C-C} = 0.142\ \text{nm}$.

Results and discussion

The analysis and the approaches to the considered nanotubes are thoroughly described and discussed concerning CNT_1, CNT_2, and CNT_3, as well as to CNT-3.

For each CNT other than the narrowest reported one of $d_k = 4\text{Å}$, it holds that it is metallic if and only if it satisfies the condition $\text{MOD}(2m+n,3) = 0$. To date, the determination of the molecular geometric structure of carbon nanotubes and its analysis has been quite challenging, even for undetermined SWCNTs, particularly for MWCNTs. Each of the four nanotubes CNT_1, CNT_2, CNT_3, and CNT-3 is undetermined concerning its diameter, chirality, and the number of walls.

This research is focused on the determination of both their innermost and outermost diameters denoted by d_i and d_o correspondingly. The determination of chiral indices (*m*,*n*), the total number and conductive nature of other inner walls having a diameter d_k, and the interlayer distance δ_r^k (Fig. 1) are usually within the interval $0.32\ \text{nm} \le \delta_r^k \le 0.35\ \text{nm}$. However, it can sometimes vary from $0.27\ \text{nm}$ up to $0.35\ \text{nm}$ (Kharissova et al., 2014).

Figure 1
Diameters of MWCNTs

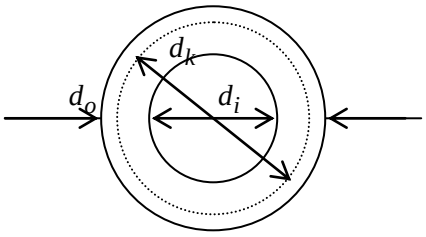

Source: Author´s work

The relation among the diameters and the interlayer distances is given by $\delta_r^k = \frac{d_k - d_{k-1}}{2}$, whereas $N = \frac{d_o - d_i}{2\delta_r} + 1$ describes the relation among the number of layers *N*, the innermost diameter d_i, the outermost diameter d_o, and the average interlayer distance δ_r.

The key role in the analysis was assigned to the Raman spectra in two frequency regions of each nanotube sample: $\omega \in [50\ \text{cm}^{-1}, 350\ \text{cm}^{-1}]$ $\omega \in [1200\ \text{cm}^{-1}, 1800\ \text{cm}^{-1}]$. The first region was expected to point to the Radial breathing mode (RBM) frequencies for SWCNTs or to Radial breathing-like mode frequencies (RBLM) for MWCNTs. These measurements can be an excellent tool to estimate the diameters of each layer of the tubes since RBM is an active mode where all carbon atoms move in phase in the radial direction. To date, several experimental relations have been established between the diameter of the tube and the RBM frequency ω_{RBM}. This work uses two equations (2.6) and (2.7), depending on the studied samples Raman data, since those relations are equivalent only within a limited range of

diameters. While (2.6) shows the dependence of the innermost diameter d_i and the outermost diameter d_o on the corresponding frequencies and is more accurate when small diameters are considered, (2.7) can be used for a much larger range of diameters and is more useful when it comes to very large diameters (or extremely low frequencies). Hence it will be used whenever relation (2.6) is unusable or unreliable due to the size of the outermost diameter. One may notice that d_i is obtained by the same equation as d_o, with C_e being 0. The latter is because the parameter C_e is used whenever environmental conditions surround the nanotube. The innermost concentric nanotube within the MWCNT is not affected by such conditions, which is not the case with the outer concentric tube. Obtaining possible (*m*,*n*) candidates to satisfy equation (2.2) and the number of these pairs was performed using Python programming for the nanotubes CNT1, CNT2, CNT3, and the Mathematica software for CNT-3. The final choice of (*m*, *n*) assignment is made by analyzing the G-peak.

The high-frequency G-mode region, showing off in the interval $\omega \in (1500\ \mathrm{cm}^{-1}, 1600\ \mathrm{cm}^{-1})$, is used to help the overall analysis. In Fig. 2, D and G-modes of the studied samples are presented. Regarding the G-mode only, a useful diameter dependence for the chiral CNTs (semiconducting or metallic), which was here used as a control method, is given by the equations (2.8) and (2.9) (Telg et al., 2012; Popov et al., 2006).

Figure 2
Raman spectra D and G-mode for CNT_1, CNT_2, and CNT_3

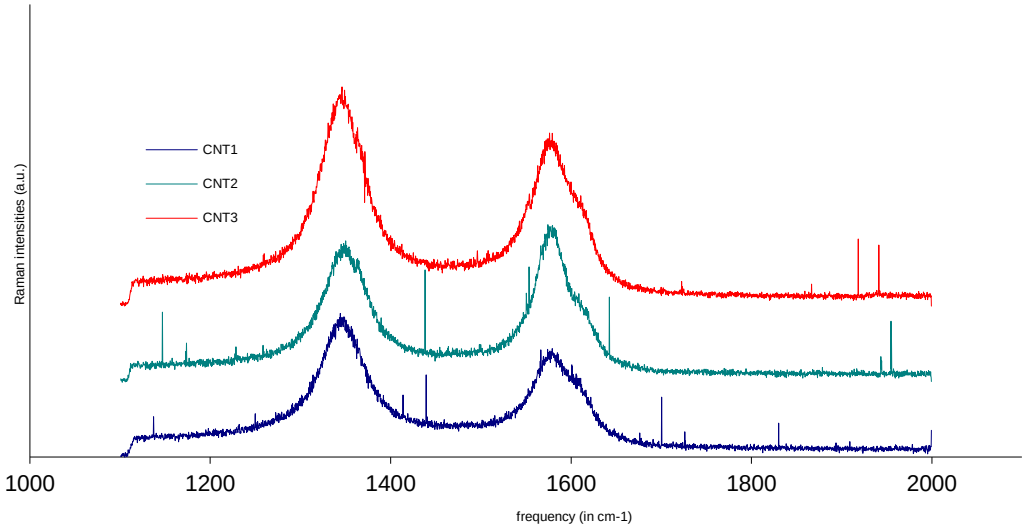

Source: Author´s work

The number and shape of components in the G-peak are excellent indicators of the conductive nature of the studied CNT sample. Table 1 will help the analysis when the chiral indices assignment to the samples is done.

Table 1
Dependence between G-peak components and the CNT conductivity

Nanotube conductivity	Components number	G-peak profile
Semiconducting chiral (SC)	2	LO: narrow, symmetric TO: narrow, symmetric
Metallic chiral (MC)	2	LO: broad, asymmetric TO: narrow, symmetric
Armchair	1	TO: narrow, symmetric
Semiconducting zig-zag (SZ)	1	LO: narrow, symmetric
Metallic zigzag (MZ)	1	LO: broad, symmetric

Source: Author´s work

Nanotube CNT_1 (m,n) assignment results

The Raman spectra in both frequency regions for CNT_1 are shown in Fig. 3. A, B. There is only one peak in the low-frequency region, which indicates that the nanotube is a single wall, i.e. $d^{(1)} = d_o^{(1)}$. Using (6), it is obtained $d^{(1)} = d_o^{(1)} = 0.665\,\text{nm}$.

Figure 3
A) Raman spectrum RBM for CNT_1 B) Raman spectrum G-mode for CNT_1

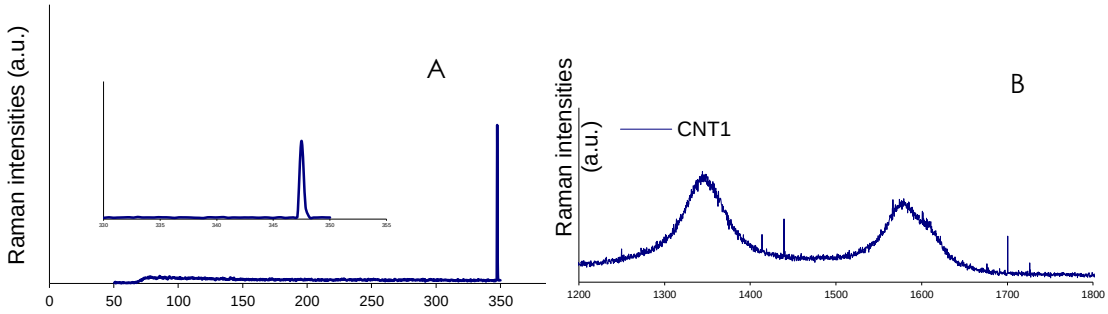

Source: Author´s work

The determined diameter is lower than 1 nm, and the most accurate results are expected for diameters 1 nm – 2.5 nm; hence the determining possible chiral indices candidates was performed within a somewhat broader diameter interval $(d^{(1)} - 0.02, d^{(1)} + 0.02)$. Python programming was applied to obtain possible candidates, and the 24 possibilities are indicated in Table 2.

Table 2
Possible (*m*, *n*) assignments for the diameter $d^{(1)} = 0.665\,\text{nm}$ of CNT_1

(4,3)	(4,4)	(5,2)	(5,3)	(5,4)	(5,5)
(6,0)	(6,1)	(6,2)	(6,3)	(6,4)	(6,5)
(6,6)	(7,0)	(7,1)	(7,2)	(7,3)	(7,4)
(7,5)	(8,0)	(8,1)	(8,2)	(8,3)	(8,4)

Source: Author´s work

Due to the broadness of the G-peak (see Fig. 3. B), the chiral indices candidate pairs need to satisfy the metallic condition $\text{MOD}(2m+n,3) = 0$. Hence, only the five chiral indices pairs in red (see Table 2) are considered. However, the armchair type (5,5) would show one narrow and symmetric G-peak, and the chiral metallic (6,3),

(7,1), and (8,2) would show two components of the G-peak, one being narrow (see Table 3.2), which here is not the case.

This leaves only one possibility, the zig-zag metallic tube (6,0), which is in high accordance with the broad and asymmetric G-peak of the nanotube CNT_1.

Nanotube CNT2 (m, n) assignment results

The Raman spectra in the RBLM frequency region and in the G-mode region for CNT_2 are shown in Fig. 4 A, B. Two peaks in the low-frequency range identify the CNT_2 as double-wall CNT (DWCNT).

Figure 4

A) Raman spectrum RBLM for CNT_2; B) Raman spectrum G-mode for CNT_2

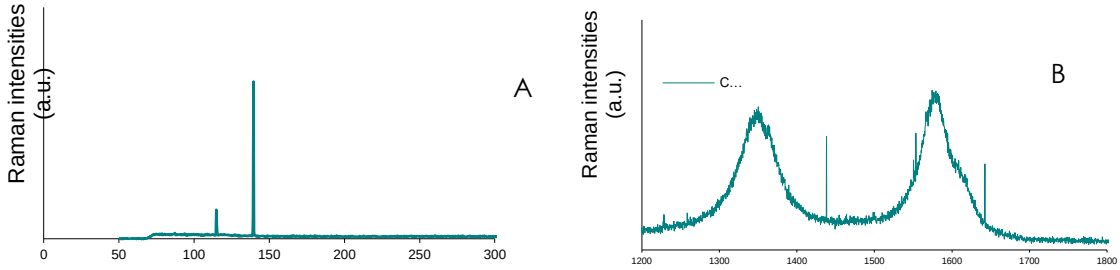

Source: Author´s work

According to the corresponding frequency values in Fig.4 A and equation (2.6), the innermost and outermost diameters are calculated as $d_i^{(2)} = 1.63\,\text{nm}$ and $d_o^{(2)} = 2.3\,\text{nm}$.

The interlayer distance is calculated as $\delta_r = \frac{d_o - d_i}{2} = 0.335\,\text{nm}$ which accurately fits the equilibrium distance for tubes that are DWCNTs.

Concerning the G-peak and the chirality of each constituent SWNT, one expects to observe 4 (Ch@Ch), 3 (Ch@ACh or ACh@Ch), or 2 (ACh@ACh) components in the Raman spectrum data of any DWNT. However, some components can appear at very close frequencies and cannot be easily differentiated. Hence, the number of observed components can be less than expected for certain sample structures (see Table 1). Considering CNT_2, two identified components of the G-peak are located at frequencies 1570.98 cm^{-1} and 1574 cm^{-1}. These frequencies enable the estimating of the diameters. Consequently, the following was obtained: $d_i^{(2)} = 1.58\,\text{nm}$ by using equation (2.8), which implicates a semiconducting chiral (SC) layer, and $d_o^{(2)} = 2.25\,\text{nm}$ by using equation (2.9), which implicates a metallic chiral (MC) layer. One may notice that the obtained diameters by both methods are in high accordance, and the values obtained by (2.6) are kept accurate.

The determined diameters are within 1 nm – 2.5 nm; hence the interval for calculating possible chiral indices candidates was performed within a narrower diameter interval with a 0.01 nm error bar $(d^{(2)} - 0.01, d^{(2)} + 0.01)$. Python programming was applied to obtain possible assignment candidates for both diameters to satisfy equation (2.2), and the results of 16 combinations are derived from the pairs indicated in Table 3.

Table 3
Possible (*m*,*n*) assignments for the innermost and outermost diameters of CNT_2

$d_o^{(2)}$	$d_i^{(2)}$
(22,11)	(12,12)
(25,7)	(13,11)
(27,4)	(17,6)
(28,2)	(19,3)

Source: Author´s work

Qualitative analysis of the G-peak indicated a broad component, hence a metallic chiral character of one layer and a semiconducting chiral character of the other layer. Hence, the possible cases are either MC@SC or SC@MC, corresponding to the implications from equations (2.8) and (2.9) results. The only chiral indices pair satisfying the MC condition is (25,7). There are three possibilities of type SC@MC: (13,11)@(25,7), (17,6)@(25,7), and (19,3)@(25,7). These three possibilities' exact innermost and outermost diameters give interlayer distances of 0.329 nm, 0.335 nm, and 0.335 nm, correspondingly. The latter eliminates the first tube, and the remaining two possibilities (17,6)@(25,7) and (19,3)@(25,7) are equally possible up to this point. However, it is possible to make a strong distinction between these two possibilities by an additional method of performing and analyzing an EDP of the CNT_2. The authors suggest further research since this analysis would estimate the ratio *m*/*n*, which greatly differs between the two possibilities. It is expected that it would leave only one candidate combination.

Nanotube CNT3 (m,n) assignment results

Several (six) peaks may be noticed in the Raman spectrum in the RBLM frequency region of CNT_3 (Fig. 3.3.1 A), which identifies this nanotube as MWCNT. The presence of both narrow and broad components in the G-mode range (Fig. 3.3.1 B) implicates both the semiconducting and metallic layers in the structure of CNT_3. According to the corresponding frequency values in Fig. 5 A and equation (2.6), the innermost and outermost diameters are calculated as $d_i^{(3)} = 0.65\ \text{nm}$ and $d_o^{(3)} = 7.73\ \text{nm}$.

The frequency of the outermost diameter $d_o^{(3)}$ is extremely low and near the limit of possible calculation; therefore, its calculation may have a high error bar or even be highly inaccurate. Hence, the outer diameter is recalculated using equation (2.7) it is obtained $d_o^{(3)} = 4.04\ \text{nm}$.

Figure 5
A) Raman spectrum RBLM for CNT_3; B) Raman spectrum G-mode for CNT_3

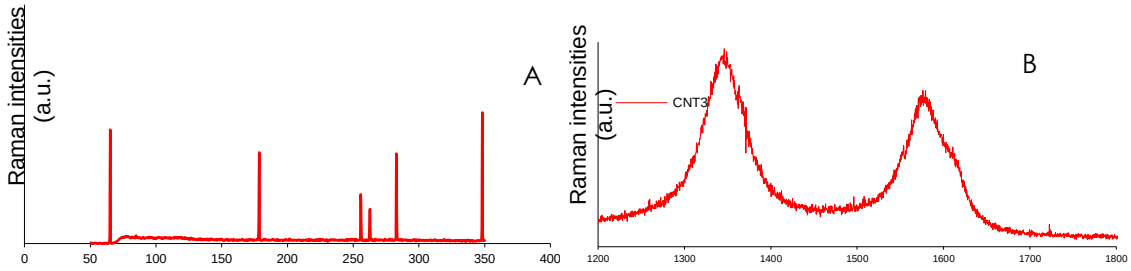

Source: Author´s work

Equation (2.8) is applied for the G-peak component frequency to decide which outermost diameter value is good. Thus, it is obtained $d_o^{(3)} = 4.07\ \text{nm}$. The latter follows the calculated value by (2.7). Furthermore, the use of this equation points to a semiconducting chiral layer. It is possible to estimate whether the choice of these equations was justified by checking the accordance with $N = \frac{d_o - d_i}{2\delta_r} + 1$ when calculating the average interlayer distance δ_r in CNT_3. Using the values N=6, $d_o^{(3)} = 4.04\ \text{nm}$, and $d_i^{(3)} = 0.65\ \text{nm}$, hence obtaining $\delta_r = 0.339\ \text{nm}$, is an excellent indicator that the diameters are well estimated. The innermost and the outermost diameters are out of the high accuracy diameter range of 1-2.5 nm and obtained by different equations. The possible (*m*,*n*) assignment was performed using Python programming, equation (2.2), and corresponding error bars. For the outermost diameter, there were three possibilities in the interval $(d_o^{(3)} - 0.002, d_o^{(3)} + 0.002)$: (31,28), (32,27), and (49,4), each being chiral. However, considering the semiconducting nature of this layer, the only pair of chiral indices satisfying the condition $\text{MOD}(2m+n,3) \neq 0$ is (32,27).

Concerning the innermost diameter, the possible (*m*,*n*) assignment was performed in the interval $(d_i^{(3)} - 0.02, d_i^{(3)} + 0.02)$ resulting in two possibilities: (7,2) and (8,0), for which it must be emphasized that the pair (7,2) is within a much lower error bar. Both of these possibilities point to a semiconducting layer.
There are two possible combinations: (7,2)@@(32,27) and (8,0)@@(32,27). Option (7,2)@@(32,27) was discussed to be within a smaller error bar, and also its calculated interlayer distance of 0.340 nm is closer to the determined $\delta_r = 0.339\ \text{nm}$ than the distance of 0.341 nm that holds for the option (8,0)@@(32,27). However, these findings are not enough of a discrepancy at the latter option for it to be excluded.

Considering this nanotube CNT_3 it is again strongly suggested an additional EDP analysis be performed. This would differentiate the two candidates since they have different *m*/*n* ratios of the innermost constituent tubes. Hence, it is highly expected that the EDP would leave only one possible candidate.

Nanotube CNT-3 topological indices evaluation

The CNT sample considered for this study, having a nomenclature CNT – 3, is a multi-wall tube, having an outermost diameter estimated to ~ 30 nm and a length of ~ 5 μm (Fig. 3.4.1 A). Fig 3.4.1 B shows its D and G modes as part of its Raman spectrum. The ratio of their intensities I_D/I_G = 0.296 is very low, which points to its highly ordered structure, in contrast to the other three considered samples. Furthermore, the G-mode having two components (G^- and G^+) being both narrow and symmetric identify the studied CNT as a semiconducting chiral. The latter is used to narrow down the choice of the most probable chiral indices (*m*, *n*) assignment, as it must be satisfied $\text{MOD}(2m+n,3) \in \{1,2\}$ (Dresselhaus et al., 2005).

Figure 6

A. SEM and TEM images of produced CNTs; B. Raman D and G-modes display of CNT – 3.

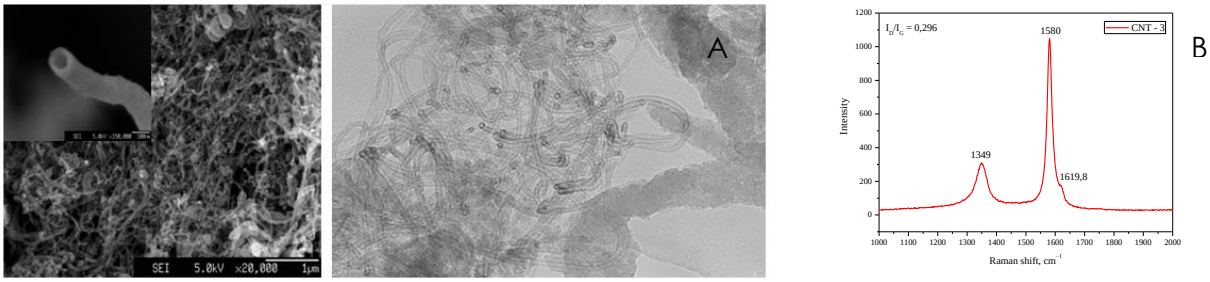

Source: Author´s work

Table 4

Possible (m, n) assignment for CNT - 3 with estimated diameter d (in nm)

d (nm)	*A* (pm^2)	(*m*, *n*)	$\tilde{A}$ (pm^2)	MOD	Cond. type	d (nm)	*A* (pm^2)	(*m*, *n*)	$\tilde{A}$ (pm^2)	MOD	Cond. type
25	101943	(295,44)	101941	1	SC	**30**	146798	(377,12)	146797	1	SC
		(261,95)	101941	2	SC			(311,117)	146797	1	SC
26	110261	(312,37)	110257	1	SC			(267,172)	146797	1	SC
		(253,123)	110257	2	SC			(283,153)	146797	2	SC
		(249,128)	110257	2	SC			(273,165)	146799	0	MC
		(207,176)	110257	2	SC			(260,180)	146800	1	SC
27	118906	(234,162)	118908	0	SC	**31**	156747	(239,218)	156747*	0	SC
28	127877	(320,66)	127876	1	SC	**32**	167023	(379,54)	167023*	2	SC
		(304,90)	127876	2	SC	**33**	177625	(347,122)	177627	0	SC
29	137174	(347,43)	137179	2	SC	**34**	188553	(419,29)	188553*	0	SC.
		(297,118)	137179	1	SC	**35**	199808	(358,143)	199807	1	SC
								(447,0)	199809	0	MZ.
*By * are denoted the exact matches of* $\tilde{A}$ *to* A.											

Source: Author´s work

The obtained results are summarized concerning the closest values of $\tilde{A} = m^2 + n^2 + mn$ to $A = \left(\frac{d}{78.3}\right)^2 (\pm 2\text{pm}^2)$ [1] and presented in Table 4 above.

Possible assignments are considered concerning $|\tilde{A} - A| < 2$ non-metallic and diameters closest to 30 nm. Based on these results, seven possible chiral indices assignments out of 23 satisfy each condition. However, it should be stressed that (379,54) is the most probable assignment, as it is the only chiral semiconducting CNT precisely satisfying $|\tilde{A} - A| = 0$.

The number of vertices/atoms in the nanotube is highly important to evaluate distance-based topological indices. The vector (m,n) determines the diameter of the tube, but the distance between any two vertices depends on the length of the nanotube and its unit cell. Using the length and the type of the nanotube, the number of vertices is asymptotically determined. The length of the translation vector $T = |\vec{T}|$ given by (2.4) and the nanotube length determine the number of (repeating) unit cells and hence the total number of vertices *N*. It is important to notice that it is possible to obtain the topological indices for the unit cell itself only and use them for

further research whenever the length of the nanotube is unknown for any reason. The obtained results are presented in Table 5.

Table 5
Summarized topological indices results for CNT – 3

d (in nm)	(m,n) assignment	$W(G)\cdot10^{19}$	$J(G)$	$SJ(G)\cdot10^{11}$	$H(G)\cdot10^{-5}$	$Gut(G)\cdot10^{20}$
28	(320,66)	6.31423	110.2	1.57031	10.35245	3.78854
28	(304,90)	6.18602	111.3361	1.60286	10.56701	3.71161
30	(377,12)	7.6744	110.6274	1.69965	9.75086	4.60464
30	(311,117)	6.9751	116.0405	1.87005	10.72846	4.18506
30	(267,172)	6.80032	117.5222	1.91811	11.00419	4.08019
30	(283,153)	6.84711	117.12	1.905	10.92899	4.10827
32	(379,54)	5.02548	103.8807	1.23514	10.32512	3.01529

Source: Author´s work

Conclusion

Based on the analysis and discussions in previous sections, it is achieved by determining the molecular structure and hence full properties of MWCNT samples mainly through Raman spectroscopy data and Python programming. Although limitations occur in some cases, particularly if the research subject is nanotubes with more than two layers, the achievement of solely using one main tool (Raman spectroscopy) is indeed outstanding. Several important findings may be concluded:

- Determination of four CNTs' molecular structure has been performed, as well as determination of the conductive nature of the CNTs' walls; fully for CNT_1 and CNT_2, and partially for CNT_3 and CNT-3;
- The thorough analyses were made using a unique approach combining the CNTs' Raman spectra in RBLM and G-mode frequency regions as a Python programming tool. The results, although with some limitations, enable working on determining structural characteristics of carbon nanotubes when there is just Raman spectroscopy data available;
- The performed calculations were in excellent agreement with the theoretical background and with the control methods;
- The calculations can be further improved in terms of higher certainty and result exactness; therefore, corresponding methods, such as EDP, are strongly suggested;
- The results provide full necessary information for graph theorists who work on distance-based topological indices, such as Wiener, Harary, Balaban, Sum-Balaban, Gutman, etc.;
- Several methods and techniques have been combined to enable and propose the approach presented on the CNT – 3 for determining its chiral indices assignment and distance-based topological indices. It is evident by the results that the determined indices distinguish the nanotubes concerning their chirality and hence open a wide research area for finding which properties of the nanotube molecules could correspond to evaluated topological indices;
- Obtained results enable many applications of CNTs and this characterization method, including the application of produced and characterized CNTs within mosquito-repellent products and procedures containing mosquito-

repellent features, such as water treatments and approaches employing characterized carbon nanomaterials.

Table 6
Summarized results to specify studied CNTs

Parameters in nanotube	CNT1	CNT2	CNT3	CNT-3
Chiral indices (m,n)	(6,0)	(17,6)@(25,7) (19,3)@(25,7)	(7,2)@@(32,27) (8,0)@@(32,27)	-@@(379,54)
Diameters (in nm)	0.665	1.63@2.3	0.65@@4.04	32
Interlayer distances (in nm)	-	0.335	0.34	-
Number of walls	1	2	6	85-95
Conducting nature	MZ	SC@MC	SC@@SC (intrinsically Metallic)	-@@SC
Chiral angles (in rad)	0	0.25@0.21 0.13@0.21	0.21@@0.47 0@@0.47	-@@0.12
Length of the unit cell (in nm)	0.6	8.87@4.17 8.87@4.17	3.54@@21.98 0.44@@21.98	@@174.12
Number of hexagons in the cell	12	854@566 854@566	134@@5234 16@@5234	@@334046
Number of vertices in the cell	24	1708@1132 1708@1132	268@@10648 32@@10648	@@668092
Total number of vertices	-	-	-	@@19184815

Source: Author´s work

References

1. Andonovic, B., Ademi, A., Grozdanov, A., Paunović, P., Aleksandar T. Dimitrov. (2015), "Enhanced model for determining the number of graphene layers and their distribution from X-ray diffraction data", Beilstein J. Nanotechnol, Vol.6, pp. 2113-2122.
2. Andonovic, B., Andova, V., Atanasova, Pacemska, T., Paunovic, P., Andonovic, V., Djordjevic, J., Dimitrov, A. (2020), "Distance based topological indices on multi-wall carbon nanotubes samples obtained by electrolysis in molten salts", BJAMI, Vol.3 No.1, pp. 7-12.
3. Andova, V., Knor, M., Škrekovski, R. (2016), "Distances on nanotubical structures", Journa of Mathematical Chemistry, Vol.54, pp. 1575-1584.
4. Balaban, A.T. (1982), "Highly discriminating distance based numerical descriptor", Chemical Physics Letter, Vol.89, pp. 399-404.

5. Balaban, A.T. (1983), "Topological indices based on topological distances in molecular graphs", Pure and Applied Chemistry, Vol.55, pp. 199-206.
6. Balaban, A.T. (2002), A comparison between various topological indices, particularly between the index J and Wiener index W in: D. H. Rouvray, R. B. King (Eds.), Topology in Chemistry Discrete Mathematics of Molecules, Horwood, Chichester, 89-112.
7. Benoit, J. M., Buisson, J. P., Chauvet, O., Godon, C., Lefrant, S. (2002), "Low-frequency Raman studies of multi-walled carbon nanotubes: Experiments and theory", Physical Review B, Vol.66 No.7, pp. 073417.
8. Devillers, J., Balaban, A.T. (1999), "Topological Indices and Related Descriptors in QSAR and QSPR", Gordon & Breach, Amsterdam.
9. Dresselhaus, G., Dresselhaus, R. Saito, A. Jorio. (2005), "Raman spectroscopy of carbon nanotubes", Physics Reports, Vol. 409, pp. 47–99.
10. Grassy, G., Calas, B., Yasri, A., Lahana, R., Woo, J., Iyer, S., Kaczorek, M., Floc'h, R., Buelow, R. (1998), "Computer-assisted rational design of immunosuppressive compounds", Nature Biotechnology, Vol.16, pp. 748-752.
11. Ivanciuc, O., Balaban, T.S., Balaban, A.T. (1993), "Design of topological indices, part 4, reciprocal distance matrix, related local vertex invariants and topological indices", Journal of Mathematical Chemistry, Vol.12, p. 309-318.
12. Khadikar, P.V., Supuran,C.T., Thakur, A.,Thakur, M. (2004), "QSAR study on benzene-sulphonamide carbonic anhydrase inhibitors: topological approach using Balaban index", Bioorganic and Medicinal Chemistry, Vol.12, pp. 789-793.
13. Kharissova, O.V., Kharisov, B.I. (2014), "Variations of interlayer spacing in carbon nanotubes", RSC Advances, Vol.4, pp. 30807-30815.
14. Natsuki, T., G.J.H. Melvin & Q.-Q. Ni. (2013), "Vibrational Frequencies and Raman Radial Breathing Modes of Multi-Walled Carbon Nanotubes Based on Continuum Mechanics", Journal of Materials Science Research, Vol.2 No.4.
15. Plavšić, D., Nikolić, S., Trinajstić, N., Mihalić, Z. (1993), "On the Harary Index for the Characterization of Chemical Graphs", Journal of Mathematical Chemistry, Vol.12, pp. 235-250.
16. Popov, V., Lambin, P. (2006), "Radius and chirality dependence of the radial breathing mode and the G-band phonon modes of single-walled carbon nanotubes", Physical Review B, Vol.73, pp. 085407.
17. Qin, L., Zhao, X., Hirahara, K., Miyamoto, Y., Ando, Y., Iijima, S. (2000), "The smallest carbon nanotube", Nature, Vol. 408, p. 50.
18. Schwandt, C., Dimitrov, A.T., Fray, D.J. (2012), "High-yield synthesis of multi-walled carbon nanotubes from graphite by molten salt electrolysis", Carbon, Vol.50, pp.1311–1315.
19. Telg, H., Duque, J. G., Staiger, M., Tu, X., Hennrich, F., Kappes, M. M., Zheng, M., Maultzsch, J., Thomsen, C., Doorn, S. K. (2012), "Chiral index dependence of the G+ and G- Raman modes in semiconducting carbon nanotubes", ACS Nano, Vol.6, pp. 904-911.
20. Wiener, H. (1947), "Structural determination of paraffin boiling points", Journal of Amerian Chemical society, Vol.1, pp. 17-20.
21. Zhao, X., Ando, Y., Qin L.-C., Kataura, HManiwa,, Y. and Saito, R. (2002), "Radial breathing modes of multi-walled carbon nanotubes", Chemical Physics Letters, Vol. 361, pp.169–174.

About the authors

Viktor Andonovic is a PhD student in ICT and a young researcher at Jožef Stefan Institute,Ljubljana, Slovenia. He is working on develpment of decision support systems for Public Employment Services, including advanced models based on machine learning and graph theory. He has completed several Short-Term Scientific Missions financed by EU H2020 projects and is an author of scientific articles published in relevant journals. The author can be contacted at: **andonovic.viksa@gmail.com.**

Mimoza Kovaci Azemi is a teaching assistant at the Faculty of Geodetic Sciences and Technology, "Xasan Pristina" University, Mitrovica, Republic of Kosovo, where she has acquired her Bachelor's and Master's Degree in metallurgy in the field of materials. She is currently a Ph.D. student of Metallurgy at the Faculty of Technology and Metallurgy, Skopje, North Macedonia. The author can be contacted at: **mimoza.kovaci@umib.net**

Prof. Beti Andonovic, Ph.D., is a Full Professor at the Faculty of Technology and Metallurgy, Skopje, North Macedonia. She obtained her Ph.D. at the Faculty of Mathematics and Natural Sciences in Skopje. She is the author of many scientific articles on mathematics and mathematical modeling and its applications, as well as on management and communication skills. Prof. Andonovic presented her scientific research as an invited speaker at numerous international conferences. She has participated in many international and national projects—currently, prof. Andonovic is an MC member in the ongoing EU projects COST Actions CA16227, CA17139, and CA17140. The author can be contacted at: **beti@tmf.ukim.edu.mk**

Prof. Aleksandar Dimitrov, Ph.D., is a Full Professor at the Faculty of Technology and Metallurgy, Skopje, North Macedonia, and Head of the Department of Extractive Metallurgy. He completed postdoctoral studies at the Department of Material Science and Metallurgy, University of Cambridge, Cambridge, UK. Prof. Dimitrov is an author of more than 100 international scientific articles and has participated in many international conferences as an invited lecturer. He had numerous research and scientific missions in many Universities, including the University of Cambridge, the University of Leeds, the University of Oxford, the UK, and others. His current research focuses on nanomaterials and nanostructures, particularly synthesising graphene, MWCNTs, and other carbon nanomaterials and quality management. Prof. Dimitrov is a current MC member in EU projects COST Actions CA17139 and CA17140 and has been a leader in many international projects. The author can be contacted at: **aco2501@gmail.com**